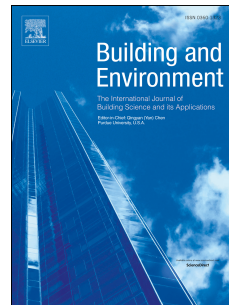


Accepted Manuscript

Fine-scale variations in PM_{2.5} and black carbon concentrations and corresponding influential factors at an urban road intersection

Zhanyong Wang, Shuqi Zhong, Hong-di He, Zhong-Ren Peng, Ming Cai



PII: S0360-1323(18)30253-1

DOI: [10.1016/j.buildenv.2018.04.042](https://doi.org/10.1016/j.buildenv.2018.04.042)

Reference: BAE 5438

To appear in: *Building and Environment*

Received Date: 31 December 2017

Revised Date: 28 April 2018

Accepted Date: 30 April 2018

Please cite this article as: Wang Z, Zhong S, He H-d, Peng Z-R, Cai M, Fine-scale variations in PM_{2.5} and black carbon concentrations and corresponding influential factors at an urban road intersection, *Building and Environment* (2018), doi: 10.1016/j.buildenv.2018.04.042.

This is a PDF file of an unedited manuscript that has been accepted for publication. As a service to our customers we are providing this early version of the manuscript. The manuscript will undergo copyediting, typesetting, and review of the resulting proof before it is published in its final form. Please note that during the production process errors may be discovered which could affect the content, and all legal disclaimers that apply to the journal pertain.

Fine-scale variations in PM_{2.5} and black carbon concentrations and corresponding influential factors at an urban road intersection

Zhanyong Wang^{a, b, *}, Shuqi Zhong^b, Hong-di He^c, Zhong-Ren Peng^{d, e}, Ming Cai^{b, *}

^a College of Transportation and Civil Engineering, Fujian Agriculture and Forestry University, Fuzhou 350002, China

^b School of Engineering, Sun Yat-sen University, Guangzhou 510006, China

^c Logistics Research Center, Shanghai Maritime University, Shanghai 200135, China

^d Center for ITS and UAV Applications Research, School of Naval Architecture, Ocean & Civil Engineering, Shanghai Jiao Tong University, Shanghai 200240, China

^e International Center for Adaptation Planning and Design (iAdapt), School of Landscape

Architecture and Planning, College of Design, Construction and Planning, University of Florida, PO
Box 115706, Gainesville, FL 32611-5706, USA

(* Corresponding authors, E-mail: wangzy1026@163.com; caiming@mail.sysu.edu.cn)

14 Abstract

Road intersections have the potential to pose an additional exposure risk to surrounding dwellers or commuters; however, knowledge of the fine-scale variations of traffic pollutants especially PM_{2.5} and black carbon (BC) remains limited. To investigate them, we conducted a three-point synchronous observation at an intersection in winter and spring. Real-time monitors with one-minute intervals were used to obtain the pollutant and meteorological data while gasoline and diesel vehicle volumes were manually collected every five minutes. Observations showed that the average PM_{2.5} on the downwind roadside increased by approximately 9% in both seasons and that the average BC increased by 70% in winter and 97% in spring compared to those of the background site. PM_{2.5} displayed a similar diurnal variation among the sites, but the BC variation was more

1 strongly correlated to the diurnal traffic cycle. Generalized additive models further identified the
2 background variation as the major contributor to the variations in both pollutants at the intersection,
3 explaining 77–99% and 33–43% of the variance in $\ln(PM_{2.5})$ and $\ln(BC)$, respectively. Air
4 pressure and solar radiation were the next top determinants of pollutant variations. Relative humidity
5 combined with air temperature in winter and with dew-point temperature in spring also had a
6 significant impact. Roadside BC was sensitive to traffic from the windward direction, while PM_{2.5}
7 was mostly influenced by the external pollution driven by westerly winds. In contrast to gasoline
8 vehicles, diesel vehicles were verified to provide an appreciable contribution of approximately 9%
9 to roadside BC variations in spring.

10 **Keywords:** Atmospheric particles; Spatiotemporal variation; Influential factor; Road intersection

11 1. Introduction

12 Traffic-related emissions have become a major driver behind the increasingly polluted air in urban
13 areas [1]. With rapid urbanization, increasingly more people tend to live, work and frequently
14 commute within the congested traffic environments of cities [2,3]. As a result, many people are
15 acutely exposed to near-road traffic pollution, which can further trigger adverse health events, such
16 as respiratory diseases and even death [4]. Due to regulatory requirements, characteristics of
17 traffic-related pollutants are typically described by urban monitoring networks with a very limited
18 number of roadside stations [5,6]. Two review articles have summarized that the air quality impact
19 of major roads is significant only within a few hundred meters [1,7]. In addition, many near-road
20 traffic pollutants have high spatial and temporal variability [1], implying that the sparse monitoring
21 networks at present cannot adequately estimate the fine-scale near-road air pollution with regard to

1 space and time. In view of the current situation, it is urgent to focus on fine-scale variations in air
2 pollutants in near-road microenvironments because this is more directly associated with human
3 exposure issues.

4 At road intersections, vehicles frequently stop with idling engines during the red-light period and
5 speed up rapidly at the commencement of the green-light period, which generates higher velocity
6 fluctuation and thus higher emission rates [9,10]. Additionally, many environmental factors, such as
7 frequently changing wind conditions, further increase the highly variable dispersion of pollutants at
8 the street scale[11-14]. In hard-hit areas of urban air pollution, it is crucial but difficult to estimate
9 the variation in pollutant concentrations near the intersection using a single roadside station.
10 Therefore, synchronous observations based on multiple points are necessary to examine the
11 near-road air quality.

12 As known, the variation in traffic pollution is mainly attributed to the coupled effects of multiple
13 factors [14-16]. For example, traffic volume and vehicular composition directly determine the
14 emission intensity of exhaust pollutants [1], while weather conditions and roadside environments
15 can change the extent of influence of traffic pollutants acting on the surrounding areas and are also
16 likely to influence the background pollution level and the spread of pollutants [17,18]. Although
17 numerous studies have discussed the impact of traffic or meteorology on the variation in air
18 pollutants in various traffic environments [1], single-factor analysis has played a leading role, and
19 the coupled effect of multiple factors has not been well addressed to date [19]. In other words,
20 before a main factor is selected for traffic pollution prevention and control, the multifactor coupling
21 process needs to be understood to accurately identify the key factors affecting the target pollutant.

1 Additionally, different metrics of traffic pollution, such as PM_{2.5} and black carbon (BC), not only
2 demonstrate their different responses to traffic variations and different near-road distribution
3 characteristics but also indicate the difference in the degree to which potential factors affect the
4 variability of target pollutants [20]. Both PM_{2.5} and BC have received increasing interest in recent
5 studies on exposure to air pollution; in urban areas, BC is recognized as a particulate pollutant that is
6 more directly related to diesel vehicles [21]. Generally, the difference of PM_{2.5} and BC associated
7 with local traffic is still not well understood [19,20,22,23]. Moreover, multiple factors, such as local
8 traffic, synoptic meteorology and sampling location, have rarely been compared in terms of their
9 coupling influences on different pollutant metrics.

10 In this study, we carried out a three-point synchronous observation experiment at a busy road
11 intersection in Shanghai, to collect field samples in both winter and spring. Then, the spatiotemporal
12 variations in PM_{2.5} and BC mass concentrations were characterized to further analyze their
13 distribution differences. Finally, the generalized additive model was introduced to reveal the
14 relationships of PM_{2.5} and BC with multiple influential factors, including the traffic volume of
15 gasoline and diesel vehicles, the meteorological indices and the pollutant background, based on
16 5-min samples from two of the measurement sites.

17 **2. Materials and methods**

18 *2.1. Field campaign and data collection*

19 Field experiments were conducted at the intersection of Humin Rd and Jianchuan Rd in the Minhang
20 District of Shanghai, China (see Fig. 1). Both Humin Rd and Jianchuan Rd were two 4-lane
21 provincial arterial roads with heavy traffic flow. The traffic flow on Humin Rd comprised gasoline

1 vehicles, including private cars and taxis, as well as light diesel vehicles, such as small- and
2 medium-sized buses or trucks, while the traffic flow on Jianchuan Rd mainly comprised heavy-duty
3 diesel vehicles, such as large-sized trucks and trailers. Both roads were heavily trafficked and
4 frequently congested, especially near the signalized intersection of the two roads. In addition, the
5 surrounding areas are densely populated with roadside residents, office workers and market traders
6 as well as crowds of commuters from and to the Jianchuan Rd station of Metro Line 5, and thus, it is
7 of great practical significance to select this area for assessing traffic pollution.

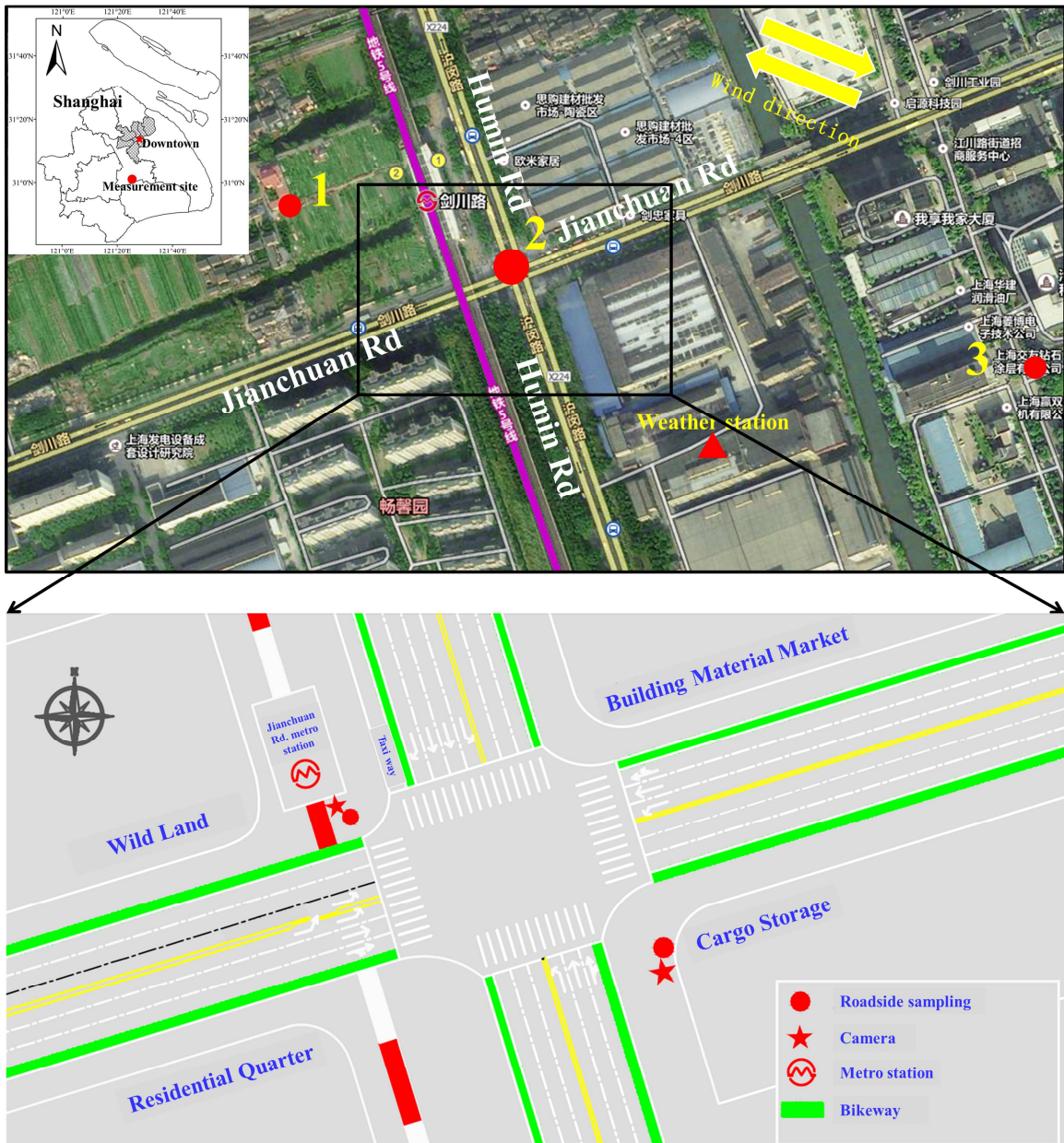


Fig. 1 Experimental layout of the three-point synchronous observation near the intersection of Humin Rd and Jianchuan Rd

As Fig. 1 shows, there are three synchronous sampling points in the study area. Point 2 was set on the roadside of the intersection (approximately 10 m from the centerline of the two adjacent roads) to reflect the direct impact of vehicle emissions on pedestrians. Because Shanghai experiences a prevailing northwest wind in winter and a southeast wind in spring, Point 2 was set southeast of the intersection in winter and northwest in spring to ensure it was always on the leeward side. Point 1

1 was set in an open area 200 m away from Point 2 to observe the influence of vehicle emissions on
2 the surrounding environment. Point 3 was located 440 m away from Point 2 so that it was far
3 enough away to serve as a background site; in addition, Point 3 sat in the center area of a science
4 park without any man-made interference or surrounding buildings, and there were no other emission
5 sources nearby. The selection of the background site was further determined from sensitivity testing
6 of the location (Ref. [24]).

7 The field campaigns lasted for 6 days in both winter and spring in 2014. Because of the accidental
8 failure and out-sync of equipment, data from 2 days were lost or invalid in winter. In total, data from
9 were available for 4 days in winter and 6 days in spring. In both seasons, the experimental days were
10 random but sunny to avoid the impacts of unusual events. The measurements of the PM_{2.5} and BC
11 concentrations started in the morning at approximately 08:00 and ended in the afternoon at
12 approximately 15:00 in winter and 18:00 in spring. Minute-by-minute PM_{2.5} concentrations were
13 collected for all three sampling sites, using a TSI SidePak AM510, which is a portable monitor with
14 light-scattering technology. With two sets of devices on hand, minute-by-minute BC concentrations
15 were collected for Point 2 and Point 3 using an AethLabs microAeth AE51, which is a lightweight
16 aethalometer that can measure the rate of change in absorption of transmitted light due to continuous
17 collection of aerosol deposit on filter. All of the devices were set at 1.7 m above the ground, which
18 was close to the breathing zone of adult pedestrians. As reported in our recent papers [24,25], all
19 monitors used here were calibrated before leaving the factory, and further estimations were made
20 using standard methods at outdoor monitoring stations in Shanghai prior to this study.

21 In this study, the traffic conditions were recorded by two cameras (Fig. 1). The valid recording time

1 was comprised of 08:00–09:00 and 11:00–14:00 in winter and 08:00–09:00, 11:00–14:00 and
2 16:00–18:00 in spring. To reduce sampling randomness, the traffic volumes were manually counted
3 over a 5-min interval, which is a relatively stable interval [26]. Vehicles can be divided into
4 categories according to their fuel types, i.e., gasoline vehicles, diesel vehicles and natural gas
5 vehicles. As shown in the *China Vehicle Emission Control Annual Report* [27], the percentages of
6 gasoline and diesel vehicles in China were 84.7% and 14.1%, respectively, in 2014. Since natural
7 gas vehicles only account for 1.2% and natural gas is a relatively clean energy, it is assumed that
8 natural gas vehicles have a negligible contribution to PM and, in particular, to BC. Here, the traffic
9 volume was divided into gasoline vehicles and diesel vehicles. Generally, in China, passenger cars
10 with 9 or fewer seats (e.g., private cars, taxis) are gasoline vehicles. Passenger vehicles with more
11 than 9 seats (e.g., buses, coaches) and freight cars (e.g., trucks, pickups, vans, and trailers) are diesel
12 vehicles. In this study, pollutant and meteorology data were unified to the timestamp of the traffic
13 series, where five continuous 1-min samples were regularized into one 5-min average.
14 Meteorological data, including air temperature (AT, °C), relative humidity (RH, %), dew-point
15 temperature (DT, °C), wind speed (WS, m/s), wind direction (WD, degree) and air pressure (AP,
16 hPa), were recorded at 1-min intervals by a Davis Vantage Weather Station. Solar radiation (SR,
17 W/m²) was recorded at the 1-min scale by a HOBO S-LIB-M003 sensor mounted on a HOBO
18 H21-002 micro-weather station only after January 19th. Weather stations were set on the roof of one
19 building in Cargo Storage approximately 220 m away from the road intersection and 25 m above the
20 ground.

21 *2.2. Traffic and meteorological variations over the experimental period*

22 Fig. 2 depicts the 5-min traffic volume across the intersection in winter and spring. The winter data

1 cover a period of 4 days, in which January 19th was Sunday and the other three days were weekdays.

2 Overall, diesel vehicles accounted for less than 20% of the total vehicles. At the morning peak, the

3 traffic volume across the intersection showed little variation between the weekdays and the weekend.

4 The spring data cover a period of 6 days, in which April 20th was a Sunday and the other five days

5 were weekdays. The total number of vehicles in the morning and evening peak periods was greater

6 than that in the midday off-peak traffic periods on weekdays. The total number of vehicles on the

7 weekend first increased and then remained unchanged, but the total number of vehicles on the

8 weekend was generally less than that on weekdays. In both winter and spring, the variation in the

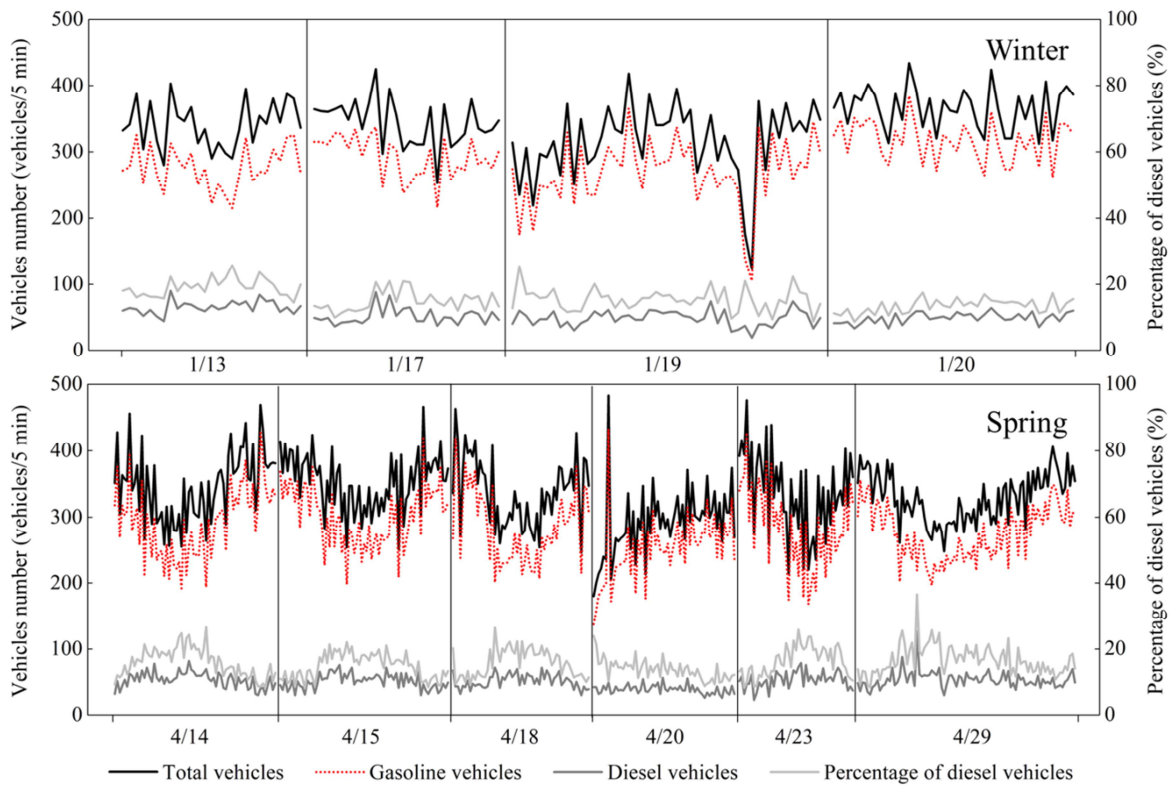
9 number of gasoline vehicles was consistent with the variation in the total number of vehicles but

10 opposite that of diesel vehicles. Moreover, the number of diesel vehicles accounted for less than 20%

11 of the total number of vehicles in peak traffic periods on weekdays and more than 20% of the total

12 number of vehicles in off-peak traffic periods on weekdays. The proportion of diesel vehicles on the

13 weekend was consistently approximately 20% and varied little with traffic periods.



1

2 **Fig. 2** The 5-min time series of the number of vehicles traveling through the Humin Rd.-Jianchuan
3 Rd. intersection

4 Table 1 shows the daily averages of the meteorological parameters recorded by the weather stations
5 near the intersection. The meteorological conditions varied considerably between seasons but
6 showed little variation for different days in the same season. On April 18th and 20th, damp weather in
7 the experimental area caused a decrease in AT and SR. Fig. 3 shows that the prevailing winds of
8 winter and spring were northwest and southeast, respectively. The mean WS in winter was 1 m/s,
9 with calm wind days accounting for 21%, while the mean WS of spring was 2 m/s, with calm wind
10 days only accounting for 6%.

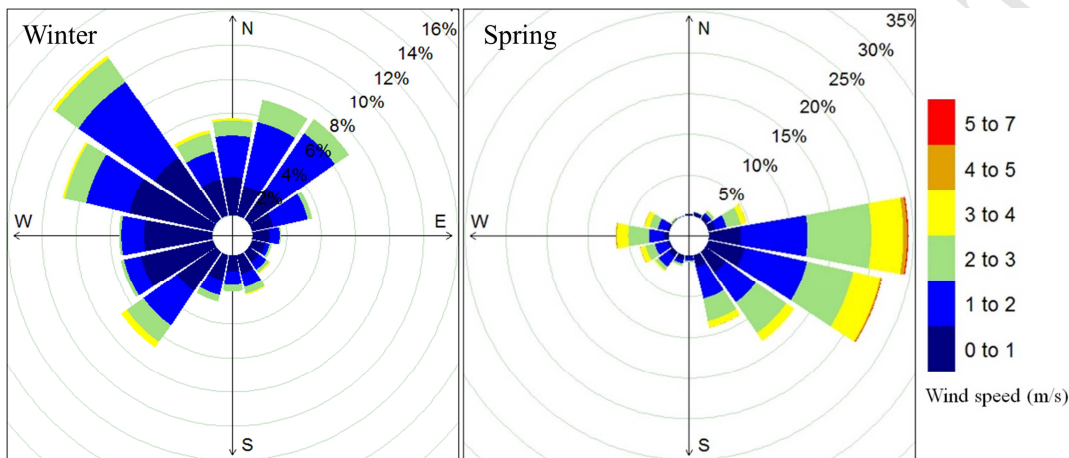
11 **Table 1** Daily averages of the meteorological parameters during the field observation experiments

Season	Date	Time period	AT (□)	RH (%)	DT (□)	WS (m/s)	WD (°)	AP (hPa)	SR (W/m ²)
Winter	1/13	9:00–15:00	6.5(0.6)	56(5)	-1.6(0.8)	1.3(0.6)	71(94)	1032.0(1.3)	n/a
	1/17	8:00–15:00	10.3(2.2)	66(12)	4.0(0.8)	0.4(0.4)	237(89)	1026.2(1.4)	n/a
	1/19	8:00–14:00	6.7(2.4)	65(10)	0.3(0.4)	1.0(0.9)	195(56)	1030.9(1.5)	512(162)
	1/20	8:00–14:00	8.3(2.4)	54(15)	-0.9(1.6)	1.3(0.9)	277(86)	1027.1(0.9)	354(121)

Spring	4/14	7:30–18:00	20.4(1.4)	53(8)	10.4(1.3)	1.6(0.9)	121(37)	1018.2(1.0)	545(305)
	4/15	7:30–18:00	20.0(1.9)	56(10)	10.5(1.3)	1.3(1.0)	128(50)	1018.8(1.7)	657(306)
	4/18	7:00–18:00	16.4(0.9)	79(4)	12.6(0.8)	2.3(1.0)	97(32)	1012.7(0.6)	207(83)
	4/20	7:00–18:00	15.8(1.0)	81(5)	12.6(0.2)	1.6(0.7)	96(17)	1014.0(1.0)	160(130)
	4/23	7:00–18:00	19.7(1.5)	39(5)	4.7(3.0)	2.0(1.0)	131(21)	1014.2(1.5)	489(255)
	4/29	7:00–18:00	21.6(2.3)	52(17)	10.5(2.9)	2.1(0.8)	253(40)	1010.4(1.3)	478(249)

1 Note: n/a represents no sample, and the number in parentheses indicates the standard deviation.

2



3

4 **Fig. 3** Wind roses over the experimental days

5 **2.3. Generalized additive model**

6 The generalized additive model (GAM) was introduced to accommodate both the linear and
 7 nonlinear relationships of the pollutants with traffic and meteorological variables. The GAM does
 8 not require any assumptions in terms of the parametric relationship between variables, which makes
 9 it an especially appealing option for the multivariate case due to the complicated nonlinearity
 10 [28-30]. In our models, the independent variables included background concentrations of PM_{2.5} and
 11 BC at Point 3; meteorological variables of AT, RH, DT, WS, WD, AP and SR; and traffic volume of
 12 gasoline and diesel vehicles. The dependent variable separately included the PM_{2.5} (or BC)
 13 concentration recorded at the near-road sites (i.e., Point 1 and Point 2) in winter or spring. The
 14 relation is described as follows:

$$\ln(PM_{2.5}) = s_1 \left(\ln(PM_{2.5}^{Bkgd}) \right) + s_2(AT) + s_3(RH) + s_4(DT) + s_5(AP) + s_6(SR)$$

$$+s_7(GVehicle) + s_8(DVehicle) + te(U, V) + \varepsilon \quad (1)$$

$$\ln(BC) = s_1(\ln(BC_{Bkgd})) + s_2(AT) + s_3(RH) + s_4(DT) + s_5(AP) + s_6(SR) + s_7(GVehicle)$$

$$2 \quad + s_8(DVehicle) + te(U, V) + \varepsilon \quad (2)$$

where $\ln(PM_{2.5})$ and $\ln(BC)$ are the natural logarithm of the PM_{2.5} and BC concentrations ($\mu\text{g}/\text{m}^3$) at the near-road sampling site, $s_i (i = 1, \dots, 8)$ is the thin-plate spline regression, te is the tensor product function, $\ln(PM_{2.5_Bkgd})$ and $\ln(BC_Bkgd)$ are the natural logarithms of the PM_{2.5} and BC background concentrations sampled at Point 3, AT is the air temperature ($^\circ\text{C}$), RH is the relative humidity (%), DT is the dew-point temperature ($^\circ\text{C}$), AP is the air pressure (hPa), SR is the solar radiation (W/m^2), $GVehicle$ and $DVehicle$ are the number of gasoline and diesel vehicles passing the intersection every 5 min (vehicles/5 min), WS and WD are the wind speed (m/s) and wind direction (rad), and ε is the residual of the GAM model.

12 The natural logarithm of the PM_{2.5} or BC concentration was used in the GAM to improve the
13 normality of the input data and residuals [30,31]. The transformation also acted to reduce the impact
14 of any outliers in the data that could skew the regression results. In the study, Pearson correlation
15 coefficients among the predictor variables mostly range from -0.35 to 0.42, indicating weak
16 correlations, but these values reached -0.58 between AT and RH in winter and 0.54 between DT and
17 AT in spring. Although these moderate correlations exist, each initial variable was included in the
18 modeling as it provided unique and irreplaceable information affecting the variation in the pollutant
19 concentrations [31]. The study also adopted the bivariate trend surface method as below to
20 characterize the strong relation between WS and WD [30].

$$21 \quad U = WS \cdot \sin(WD) \quad (3)$$

$$V = WS \cdot \cos(WD) \quad (4)$$

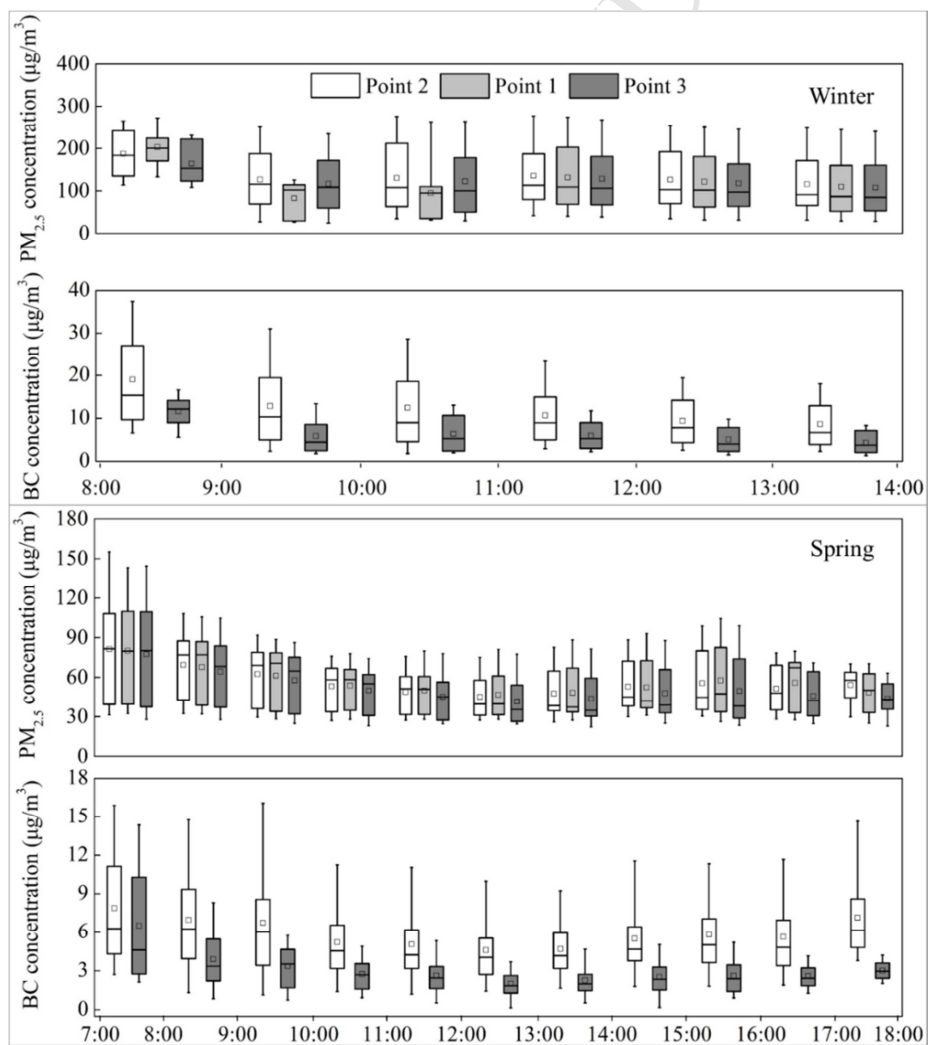
2 where $U > 0$ means the WD is east, and $V > 0$ means the WD is north. The mgcv package in R
3 Software version 3.3.3 was employed to run the GAM models. The gamm function was selected to
4 accommodate an autoregressive covariance structure in the model. The study referred to the
5 modeling steps detailed by Richmond-Bryant et al. to obtain the best model [31]. F -tests were lastly
6 used to assess the significance of the coefficient of each independent predictor in the GAM model.

7 **3. Results and discussion**

3.1. Fine-scale variations in PM_{2.5} and BC concentrations at the intersection

The three observation locations, as defined in the experimental section, present different results. The results from Fig. 4 demonstrate that the hourly averaged BC concentration was obviously higher at Point 2 than that at Point 3. Apart from several hours when Point 1 had a higher PM_{2.5} concentration than Point 2, the hourly averaged PM_{2.5} concentration was generally highest at Point 2, followed by that at Point 1, and was lowest at Point 3. The average concentration of PM_{2.5} at the roadside (Point 2) was higher than that at the background site (Point 3) by 10 µg/m³ (9%) in winter and 5 µg/m³ (9%) in spring, and for BC, the concentrations were higher by 4 µg/m³ (70%) in winter and 3 µg/m³ (97%) in spring. The three sites generally resembled each other in terms of the diurnal variation in PM_{2.5}, while the diurnal variation in roadside BC better resembled the diurnal cycle of the traffic variation. At the roadside site, the Pearson correlation coefficient between PM_{2.5} and BC was 0.6 in winter and 0.4 in spring. The BC measured at the background site was highly correlated with PM_{2.5} at all sites, and the correlation coefficient even reached up to 0.8 in both seasons. This further indicates that BC differs from PM_{2.5} with regard to space and time in the road microenvironment.

1 Using observations in spring as an example, the concentrations of both pollutants were high in the
 2 early morning and decreased gradually until the evening traffic peak. In contrast to BC, PM_{2.5}
 3 reached the peak value at approximately 03:00 pm, prior to the evening traffic peak. This finding is
 4 consistent with some previous studies on urban aerosols [20,31]. The SR often reaches its maximum
 5 at approximately 03:00 pm in Shanghai, which likely increases the secondary products of PM_{2.5}. In
 6 contrast, BC is closely related to the emission intensity, location and timing of the emission source
 7 rather than the secondary products [8]. This is also demonstrated by the greater variation in BC at
 8 the roadside than that at Point 3.



1 **Fig. 4** Boxplots of the hourly PM_{2.5} and BC concentrations measured at the sampling locations. Note:
2 The boxplot label from top to bottom separately indicates the 95th, 75th, 50th, 25th and 5th quantile;
3 the hollow dot denotes the sample mean.

4 The fine-scale variations in the pollutant concentrations at the intersection are related to traffic
5 conditions, meteorological conditions, pollutant background levels and other potential factors [14].
6 Fig. 5 shows that at the roadside, both PM_{2.5} and BC have a positive linear correlation to the road
7 traffic volumes at the intersection. In the past, Kendrick et al. suggested that traffic volume alone
8 could be well adopted as a proxy of traffic pollution exposure [33]. However, this was impracticable
9 in our study because of the weak correlations ($R=0.18\text{--}0.24$) between pollutants and traffic volumes.
10 From Table 2, meteorological conditions are correlated to different strengths with each pollutant,
11 and in general, WD, AP and SR outperform other factors in both the strength and significance of the
12 correlations. Compared with BC, PM_{2.5} shows a stronger positive correlation with WD in both
13 seasons, indicating that wind from the west or northwest can easily result in a high level of PM_{2.5}. It
14 can be further inferred that the external transport driven by the northwesterly wind, leading to the
15 high background level of the pollutants, plays an important role in the variations in PM_{2.5} at the
16 intersection.

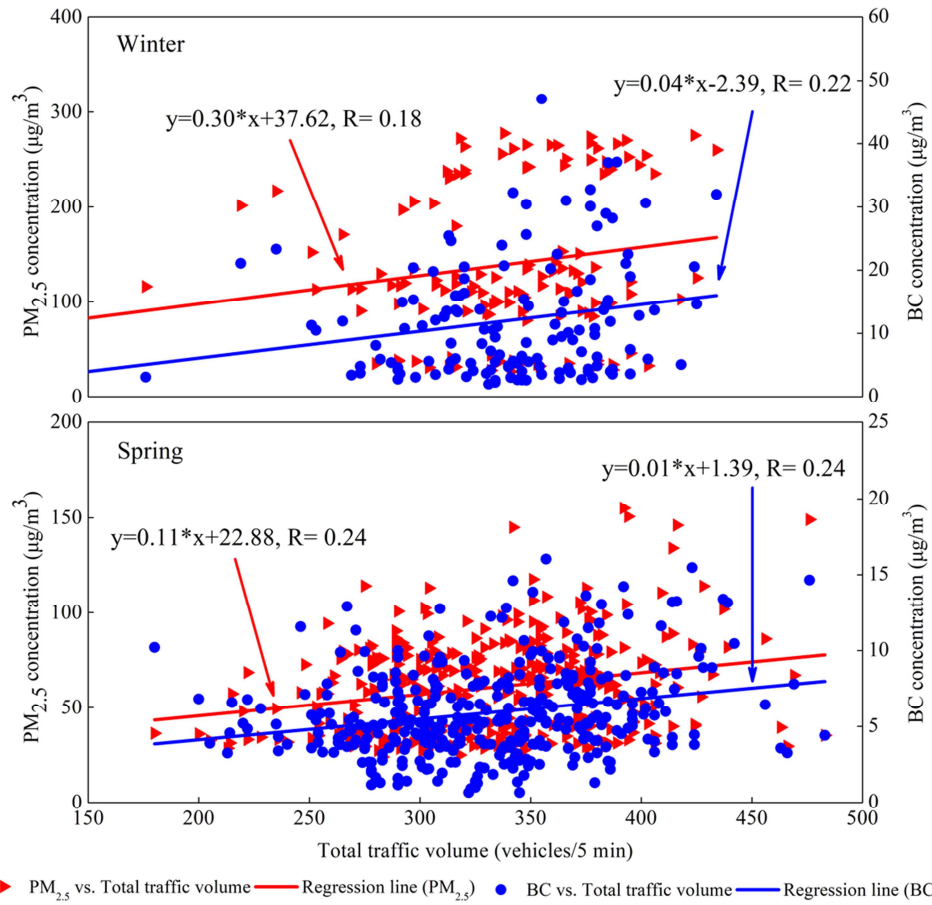


Fig. 5 Relations of both PM_{2.5} and BC at the roadside (Point 2) with the total traffic volume of the intersection. Note: Linear regressions are expressed as $y=\beta_1*x+\beta_0$, where x is the variable at the horizontal axis; y is the variable at the vertical axis; β_1 and β_0 are slope and intercept of the regression equation, respectively; and R indicates the Pearson correlation coefficient.

Table 2 Pearson correlations of PM_{2.5} and BC with meteorological conditions at the 5 min scale

Season	Pollutant	Site	AT	RH	DT	WS	WD	AP	SR
Winter	PM _{2.5}	Point 2	0.07	-0.04	-0.06	-0.04	0.73	-0.50	-0.63
		Point 1	0.09	-0.03	-0.06	-0.02	0.69	-0.48	-0.58
		Point 3	0.09	-0.10	-0.10	0.03	0.71	-0.48	-0.54
	BC	Point 2	-0.02	0.18	0.15	-0.31	0.58	-0.46	-0.79
		Point 3	-0.04	0.33	0.25	-0.38	0.65	-0.51	-0.69
Spring	PM _{2.5}	Point 2	0.21	-0.06	0.10	-0.10	0.56	-0.22	0.06
		Point 1	0.26	-0.07	0.13	-0.07	0.61	-0.26	0.09
		Point 3	0.23	-0.06	0.14	-0.07	0.63	-0.25	0.11
	BC	Point 2	-0.24	0.09	-0.04	-0.18	-0.27	0.19	-0.16
		Point 3	-0.11	0.19	0.22	-0.18	0.43	-0.17	-0.10

Note: The bold format indicates that the value is statistically significant at the 95% level (2-tailed test of significance). Correlation coefficients between the pollutants and SR in winter were calculated based on only samples from two days.

1 3.2. The impacts of the background level on $PM_{2.5}$ and BC variations

2 Considering all of the observed traffic and meteorological conditions in addition to each pollutant
 3 measured at Point 3 as independent variables, GAM models for $\ln(PM_{2.5})$ were built at Point 1 and
 4 Point 2, and GAM models for $\ln(BC)$ were established at Point 2. The performances of the
 5 well-built $\ln(PM_{2.5})$ GAM models at both sites in winter and spring were excellent. All models
 6 reached an Adj.R² of greater than 0.9 and explained more than 90% of the variance in $\ln(PM_{2.5})$ in
 7 both seasons and $\ln(BC)$ in winter. The model had a moderate Adj.R² (0.6) and explained 65% of
 8 the variance in $\ln(BC)$ in spring. In Table 3, at Point 2, $\ln(PM_{2.5_Bkgd})$ contributed more than
 9 95% of the $\ln(PM_{2.5})$ variance in both seasons, and at Point 1, it explained 77% of the $\ln(PM_{2.5})$
 10 variance in winter and 99% in spring. Although $\ln(BC_Bkgd)$ contributed the greatest part (33%)
 11 in winter and 43% in spring) of the $\ln(BC)$ variance, the contributions of RH, AP and AT to the
 12 $\ln(BC)$ variance also reached 25%, 19% and 12% in winter, respectively, and SR even contributed
 13 to 33% of the $\ln(BC)$ variance in spring. However, the GAM models did not show a significant
 14 impact from traffic volume or wind on either $PM_{2.5}$ or BC variance.

15 **Table 3** F-statistics and p-values for the F-tests of each coefficient of the $\ln(PM_{2.5})$ and $\ln(BC)$ GAM
 16 models

Season	Covariate	Point 2 / $\ln(PM_{2.5})$			Point 2 / $\ln(BC)$			Point 1 / $\ln(PM_{2.5})$		
		F-statistic	% of variance	p-value	F-statistic	% of variance	p-value	F-statistic	% of variance	p-value
Winter	s(ln(bkgd))	720.7	96.6	<0.001	18.0	33.1	<0.001	185.7	77.1	<0.001
	s(AT)	9.2	1.2	<0.001	6.5	11.9	<0.001	14.0	5.8	<0.001
	s(RH)	0.2	0.0	0.694	13.3	24.5	<0.001	25.4	10.6	<0.001
	s(DT)	0.4	0.1	0.532	2.3	4.3	0.075	4.1	1.7	<0.001
	s(AP)	3.6	0.5	0.031	10.5	19.2	0.002	4.3	1.8	0.001
	s(GVehicle)	2.5	0.3	0.410	0.1	0.3	0.704	2.6	1.1	0.055
	s(DVehicle)	5.2	0.7	0.005	1.2	2.3	0.269	3.4	1.4	0.070
	te(U,V)	4.6	0.6	0.599	2.4	4.4	0.070	1.5	0.6	0.230
Spring	s(ln(bkgd))	1294.5	99.0	<0.001	24.3	42.6	<0.001	1193.7	98.5	<0.001

s(AT)	0.0	0.0	0.878	1.0	1.8	0.495	1.7	0.1	0.199
s(RH)	1.6	0.1	0.165	0.1	0.1	0.800	4.8	0.4	0.002
s(DT)	1.7	0.1	0.191	1.5	2.6	0.184	2.2	0.2	0.060
s(AP)	2.5	0.2	0.056	4.6	8.1	<0.001	2.3	0.2	0.063
s(SR)	3.6	0.3	0.059	18.8	33.0	<0.001	4.6	0.4	0.001
s(GVehicle)	1.3	0.1	0.263	0.6	1.0	0.444	0.1	0.0	0.765
s(DVehicle)	0.1	0.0	0.764	2.6	4.5	0.048	0.6	0.1	0.423
te(U,V)	1.9	0.1	0.029	3.6	6.2	<0.001	1.4	0.1	0.150

1

2 For the PM_{2.5} measurements at the intersection, the effect of the pollutant background levels almost
 3 covered the contributions from the other variables. Although the primary contributor to roadside BC
 4 variations was the background level, traffic and meteorological parameters made significant
 5 contributions as well. Richmond-Bryant et al. performed a multisite analysis of the association
 6 between BC (or PM_{2.5}) and traffic volume, vehicular idling, pollution background, and meteorology
 7 near schools in New York, and found the PM_{2.5} background levels were the primary contributors to
 8 both $\ln(BC)$ and $\ln(PM_{2.5})$ [31]. In accordance with our findings, they concluded that $\ln(BC)$
 9 was more sensitive to traffic conditions than $\ln(PM_{2.5})$, and PM_{2.5} outperformed BC in the GAM
 10 modeling. They further attributed the low goodness of fit of their BC models to the lack of
 11 information regarding ultrafine particles, BC background concentrations, and cold start emissions
 12 for automobiles, and deemed that seasonal variations affected the model performance. The
 13 performance of the $\ln(BC)$ GAM model in our study was much better in winter than that in spring.
 14 This may be because the BC variation is aligned to meteorological changes more significantly in
 15 winter compared to that in spring (see Table 2).

16 3.3. The impacts of traffic and meteorological conditions on PM_{2.5} and BC variations

17 After removing the background variable, the Adj.R² of the rebuilt GAM models decreased relative to
 18 the GAM models that consider the background independent variable, especially in spring

(Adj.R²=0.5–0.8). Despite this, the GAM models still explained more than 90% of the $\ln(PM_{2.5})$ or $\ln(BC)$ variance in winter and 56–86% in spring. As Table 4 shows, the meteorological parameters were the predominant reason for the variance in $\ln(PM_{2.5})$ and $\ln(BC)$, among which AP was the primary contributor, while SR was also a significant contributor in spring. The combined contribution of AT and RH in winter or RH and DT in spring to the variance in $\ln(PM_{2.5})$ and $\ln(BC)$ was generally similar to that of AP and SR. The wind appeared to contribute significantly to the variance in $\ln(PM_{2.5})$ and $\ln(BC)$ at the 95% confidence level. In spring, DVehicle contributed approximately 9% to the roadside $\ln(BC)$ variance, while the contribution of GVehicle was always lower than 5% in both seasons.

Table 4 F -statistics and p -values for the F -tests of each coefficient of the $\ln(PM_{2.5})$ and $\ln(BC)$ GAM models without the background variable

Season	Covariate	Point 2 / $\ln(PM_{2.5})$			Point 2 / $\ln(BC)$			Point 1 / $\ln(PM_{2.5})$		
		F -statistic	% of variance	p -value	F -statistic	% of variance	p -value	F -statistic	% of variance	p -value
Winter	s(AT)	16.9	17.3	<0.001	5.8	2.2	<0.001	26.6	20.4	<0.001
	s(RH)	19.1	19.6	<0.001	13.6	5.1	<0.001	28.1	21.5	<0.001
	s(DT)	7.4	7.6	<0.001	2.9	1.1	0.01	9.7	7.4	<0.001
	s(AP)	48.2	49.4	<0.001	237.2	89.7	<0.001	58.6	44.8	<0.001
	s(GVehicle)	0.3	0.3	0.594	0.2	0.1	0.659	2.1	1.6	0.149
	s(DVehicle)	3.4	3.5	0.02	0.9	0.3	0.44	2.7	2.1	0.0427
	te(U,V)	2.3	2.3	0.033	3.9	1.5	0.011	2.8	2.2	0.009
Spring	s(AT)	0.8	2.8	0.502	2.0	6.3	0.163	1.3	4.0	0.272
	s(RH)	3.0	10.1	0.008	3.0	9.8	0.044	3.9	12.0	<0.001
	s(DT)	6.5	21.6	<0.001	4.4	14.2	<0.001	6.2	19.0	<0.001
	s(AP)	9.8	32.7	<0.001	5.3	17.0	<0.001	11.0	34.0	<0.001
	s(SR)	6.4	21.1	<0.001	10.8	34.7	<0.001	6.8	20.9	<0.001
	s(GVehicle)	0.2	0.6	0.672	0.7	2.3	0.399	0.3	0.9	0.599
	s(DVehicle)	0.1	0.3	0.772	2.7	8.6	0.039	0.4	1.3	0.515
	te(U,V)	3.3	10.8	0.004	2.2	7.2	0.016	2.6	7.9	0.039

1 The relationships between $\ln(PM_{2.5})$ and the variables were almost the same at Point 1 and Point 2,
 2 both in winter and spring, which were slightly different from the relationship between $\ln(BC)$ and
 3 the variables at Point 2, as shown in Fig. 6 and Fig. 7.

4 In winter, both $\ln(PM_{2.5})$ and $\ln(BC)$ decreased with increasing AP, which indicates that low AP
 5 will increase the concentrations of particulate matter near the ground. Based on 7-day field
 6 campaigns near a road in Hangzhou in winter, Jian et al. also found a negative correlation between
 7 UFP (or PM_{1.0}) and AP [34]. They explained that the rise in warm air led to low AP near the ground,
 8 and the rise in wet air caused cloud formation, which thus blocked the vertical diffusion of
 9 pollutants near the ground. In winter, when the boundary layer is low and the atmospheric structure
 10 is stable, high humidity would also accelerate the condensation, nucleation and growth of particulate
 11 matter and then increases the concentration of particulate matter. Our study observed low AP on
 12 January 17th and 20th, which only corresponded to high PM_{2.5} and BC concentrations. At that time,
 13 the wind mainly blew from the west. This implies that external pollutant transport contributed
 14 substantially to the outcome of our experiment at this intersection and that the external high AP
 15 restrained the outward diffusion of local pollutants [35]. In spring, the relationship of AP with
 16 $\ln(PM_{2.5})$ and $\ln(BC)$ showed fluctuation, which can be explained by the unstable atmospheric
 17 activity. To be specific, the interaction between the cold/warm air and cyclonic activity weakens the
 18 stability of the atmospheric structure [36]. In addition, AP coupled with AT, humidity and wind may
 19 create a more unstable atmospheric structure [34].

20 In the spring, SR was generally related to the $\ln(PM_{2.5})$ and $\ln(BC)$ variations with a negative
 21 sign. This is because high SR and low humidity accelerate the dilution and diffusion of pollutants,

1 while low SR with clouds blocks the vertical diffusion of pollutants [14]. $\ln(BC)$ decreased
 2 linearly with the increase in SR, indicating that the BC concentration decreases rapidly with high SR
 3 because SR can catalyze the photochemical reaction of BC itself such that it is largely consumed
 4 [37,38]. In contrast, there exists a stepwise relationship between the SR and $\ln(PM_{2.5})$. In
 5 particular, $\ln(PM_{2.5})$ reached a second peak when the SR went close to approximately 750 W/m².
 6 From this finding, it can be interpreted that the strong irradiation coupled with high temperature and
 7 high humidity promotes the secondary products of the photochemical reactions among O₃, NO_x,
 8 SO₂, etc. [14,39]. Then, the secondary PM_{2.5} increases the total concentration of PM_{2.5} at this time.

9 $\ln(BC)$ and $\ln(PM_{2.5})$ were significantly related with AT in winter. $\ln(BC)$ increased almost
 10 linearly with AT, while $\ln(PM_{2.5})$ increased initially and then decreased with AT. Meanwhile,
 11 $\ln(BC)$ and $\ln(PM_{2.5})$ increased with increasing RH. Jian et al. summarized that high temperature
 12 combined with high humidity facilitated the formation and chemical conversion of secondary
 13 organic aerosols [34]. Considering the negative relationship between the pollutants and AP as
 14 discussed previously, we speculate that high humidity and low pressure facilitate the nucleation and
 15 growth of particulate matter. Moreover, high humidity together with low density air always causes a
 16 decrease in the oxygen content in the air. Therefore, the combustion efficiency of a vehicle's engine
 17 is decreased, which eventually promotes particle emissions [40].

18 In the spring, the correlations of AT with $\ln(BC)$ or $\ln(PM_{2.5})$ were insignificant at the 95%
 19 confidence level; however, RH and DT had significant impacts on the variance in $\ln(PM_{2.5})$ and
 20 $\ln(BC)$. $\ln(BC)$ and $\ln(PM_{2.5})$ decreased with increasing RH and increased with increasing DT.
 21 The contribution of the DT was greater than that of RH. The diffusion conditions and impact of local

1 traffic emissions are strong in spring; as a result, high humidity will not only facilitate the growth of
 2 particulate matter but also settle particulate matter in the process of diffusion, or even restrain the
 3 photochemical reaction to create secondary particles [14]. The positive contribution of DT to
 4 $\ln(BC)$ and $\ln(PM_{2.5})$ in spring suggests that an increase in the water vapor condensation
 5 temperature indicates high humidity in the air, which will promote the creation of particulate matter
 6 and increase the concentrations of BC and PM_{2.5}.

7 Although wind provided a significant contribution to $\ln(BC)$ and $\ln(PM_{2.5})$ in both seasons, the
 8 impact in spring was stronger than that in winter overall. As can be observed in Fig. 6 and Fig. 7, the
 9 contribution of west or northwest wind to the variation in $\ln(PM_{2.5})$ at both sites was always the
 10 greatest among all WDs, while the greatest contributor for $\ln(BC)$ at the roadside was the northeast
 11 wind in winter and the east wind in spring. This further implies that PM_{2.5} at both sites was mostly
 12 influenced by the external pollution driven by westerly winds, while BC at the roadside was
 13 extremely sensitive to road traffic from the windward direction of the site. The higher sensitivity of
 14 this difference in BC relative to PM_{2.5} to direct traffic emissions in urban microenvironments has
 15 also been demonstrated in prior studies [19,31,32,41]. The contribution of gasoline and diesel
 16 vehicle emissions to $\ln(BC)$ and $\ln(PM_{2.5})$ was always less than 5% and insignificant. As an
 17 exception, the diesel vehicles had a contribution of approximately 9% to the variation in roadside
 18 $\ln(BC)$ in spring. However, there was an unstable relationship between the diesel vehicles and
 19 $\ln(BC)$ (see Fig. 7), which requires more samples to better understand.

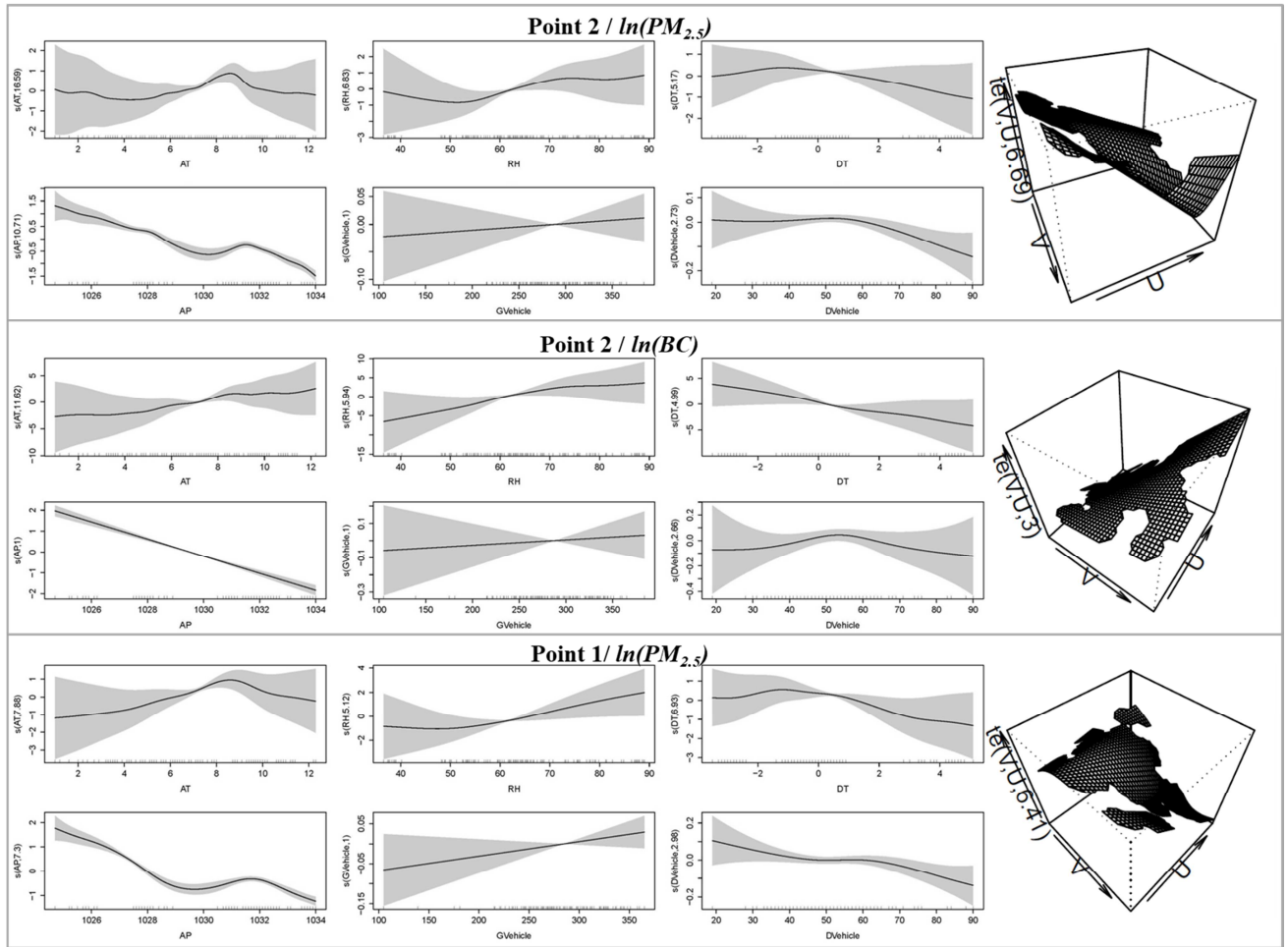
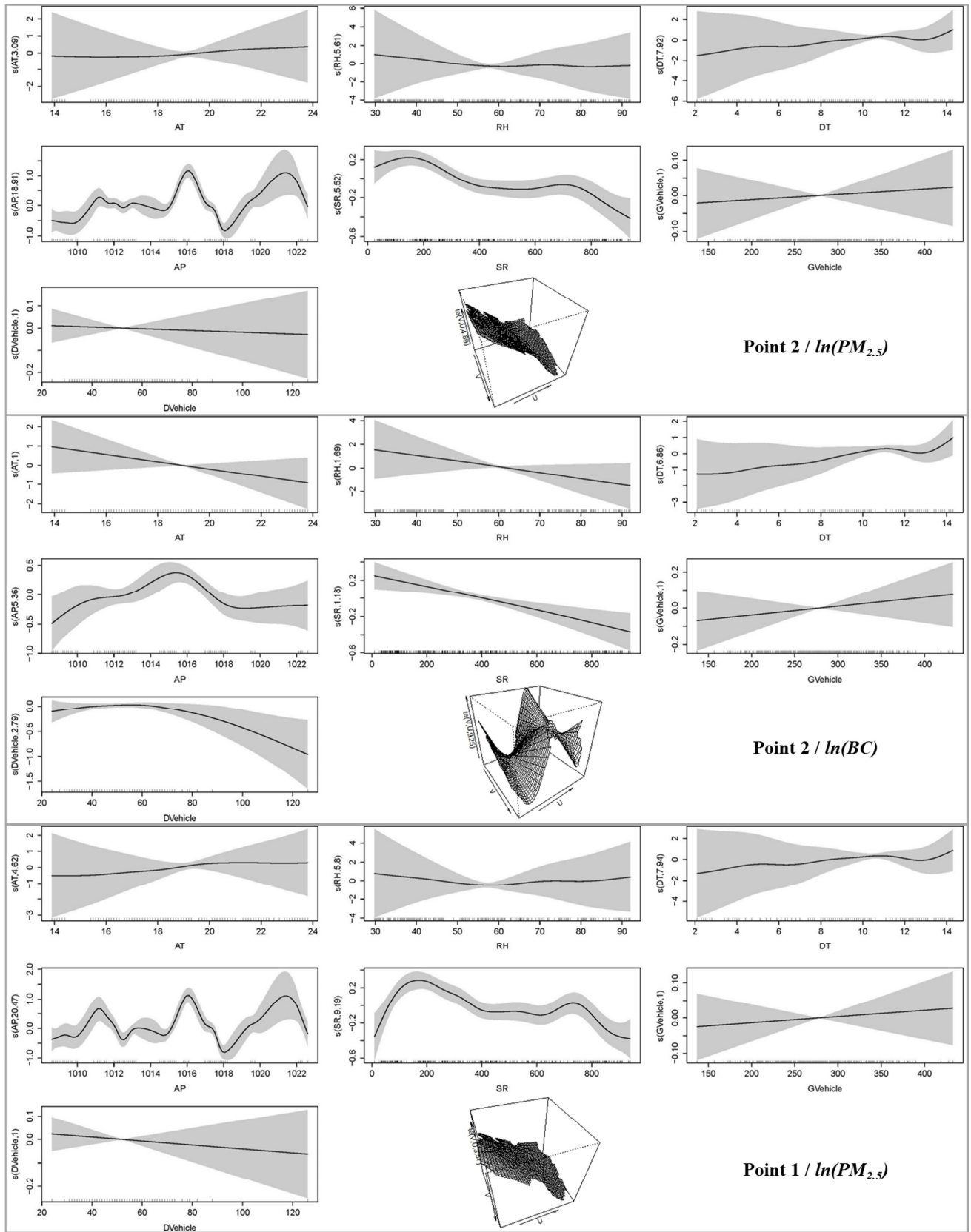


Fig. 6 Variations in the covariate smoothing functions of the $\ln(\text{PM}_{2.5})$ and $\ln(\text{BC})$ GAM models without the background variable in winter. Note: The horizontal and vertical axes of the one-dimensional graph separately indicate the independent variable and its smooth function; the gray area shows the estimate of the 95% confidence intervals, and the vertical dashes at the bottom of the plot illustrate locations where data for the plotted covariate informs the model estimates. The definitions are suitable for Fig. 7.



1

2 **Fig. 7** Variations in covariate smoothing functions of the $\ln(PM_{2.5})$ and $\ln(BC)$ GAM models
3 without the background variable in spring

1 **4. Conclusions**

2 Synchronous observations at the road intersection in Shanghai showed that the average
 3 concentrations of pollutants at the downwind roadside site were higher than those at the background
 4 site, with an average increment of $10 \mu\text{g}/\text{m}^3$ (9%) for $\text{PM}_{2.5}$ and $4 \mu\text{g}/\text{m}^3$ (70%) for BC in winter and
 5 $5 \mu\text{g}/\text{m}^3$ (9%) for $\text{PM}_{2.5}$ and $3 \mu\text{g}/\text{m}^3$ (97%) for BC in spring. $\text{PM}_{2.5}$ showed a similar diurnal
 6 variation at all sites and reached an afternoon peak value prior to the evening traffic peak. The BC
 7 variation better resembled the diurnal cycle of the traffic than did that of $\text{PM}_{2.5}$. The GAM models
 8 identified the background level as the primary contributor that explained 77–99% and 33–43% of
 9 the variance in $\ln(\text{PM}_{2.5})$ and $\ln(\text{BC})$, respectively. Besides of the background influence,
 10 meteorological conditions are also examined to be an essential role in pollutant variation.

11 The rebuilt GAM models without the background variable showed that AP and SR were the top two
 12 meteorological parameters contributing to the variance in $\ln(\text{PM}_{2.5})$ and $\ln(\text{BC})$. AP was
 13 negatively correlated with the pollutants in winter and linearly related to BC but had a fluctuating
 14 relationship with both pollutants in spring. Local low AP with external high AP in winter typically
 15 restrains the outward diffusion of local pollutants and, thus, increases the ground-level pollutants.
 16 SR in spring had a linearly negative relationship with BC but showed an undulating negative
 17 correlation with $\text{PM}_{2.5}$. This demonstrates that with increasing SR, BC is easily consumed, whereas
 18 the secondary products can slow a decrease in the $\text{PM}_{2.5}$ or even elevate the $\text{PM}_{2.5}$. Compared to the
 19 top two factors, RH combined with AT in winter or with DT in spring played a significant role in the
 20 particle variations. As seen from the impacts of winds on $\ln(\text{BC})$ and $\ln(\text{PM}_{2.5})$, the roadside BC
 21 was sensitive to the local traffic variation at the upwind location, while $\text{PM}_{2.5}$ was greatly influenced
 22 by the external pollution under a westerly wind. Meteorological conditions largely masked the

1 contribution from vehicles to the particle variations, but compared to gasoline vehicles, the traffic
2 volume of diesel vehicles still had an appreciable contribution to the roadside BC variation in spring.

3 Focusing on a hot spot of urban air pollution, this study preliminarily investigated the spatial and
4 temporal distributions of two typical atmospheric particles and their relationships with the influential
5 factors on a fine-scale scale. The results may help develop effective strategies for pollution control
6 and air quality management at roadsides. The study also has limitations. For example, the authors
7 only measured BC at two local sites due to the limited availability of equipment; sampling was also
8 further limited by the number of sample days and the degree of repetition. Future research will better
9 explain the dynamic variations in atmospheric particles by considering the driving conditions of
10 vehicles [42,43]. Hence, further research is recommended to improve these deficits.

11 Acknowledgements

12 This work is supported by the National Natural Science Foundation of China (No. 41701552 &
13 No.11672176), and the Science and Technology Project of Guangzhou, China (No. 201803030032).
14 We thank Prof. Qingyan Fu, Yusen Duan and Huxiong Cui at the Shanghai Environmental
15 Monitoring Center, Dr. Yuanxin Ge at the Min-hang District Environmental Protection Bureau, and
16 Prof. Jianmin Chen and Yang Yu at the Fudan University for their assistance in providing monitors
17 and instrumental calibration. We also express appreciation to members from the Center for ITS and
18 UAV Applications Research at Shanghai Jiao Tong University for their help in the field experiment.

19 References

- 20 [1] HEI Panel on the Health Effects of Traffic-Related Air Pollution, Traffic-related air pollution:
21 A critical review of the literature on emissions, exposure, and health Effects, HEI Special

- 1 Report 17, Health Effects Institute, Boston, MA, 2010.
- 2 [2] Z. Ning, C. Sioutas, Atmospheric processes influencing aerosols generated by combustion and
3 the inference of their impact on public exposure: a review, *Aerosol and Air Quality Research*
4 10 (2010) 43–58.
- 5 [3] L.I. Panis, B.D. Geus, G. Vandenbulcke, et al., Exposure to particulate matter in traffic: A
6 comparison of cyclists and car passengers, *Atmospheric Environment* 44 (2010) 2263–2270.
- 7 [4] C.A. Pope, M. Ezzati, D. Dockery, Fine-particulate air pollution and life expectancy in the
8 United States, *The New England Journal of Medicine* 360 (2009) 376–386.
- 9 [5] S.K. Pandey, K.H. Kim, S.Y. Chung, et al., Long-term study of NO_x behavior at urban
10 roadside and background locations in Seoul, Korea, *Atmospheric Environment* 42 (2008) 607–
11 622.
- 12 [6] K.H. Kwak, S.H. Lee, J.M. Seo, et al., Relationship between rooftop and on-road
13 concentrations of traffic-related pollutants in a busy street canyon: Ambient wind effects,
14 *Environmental Pollution* 208 (2016) 185–197.
- 15 [7] Y. Zhou, J.L. Levy, Factors influencing the spatial extent of mobile source air pollution
16 impacts: a meta-analysis, *BMC Public Health* 7 (2007) 89.
- 17 [8] R. Bahadur, P.S. Praveen, Y. Xu, et al., Solar absorption by elemental and brown carbon
18 determined from spectral observations, *Proceedings of the National Academy of Sciences* 109
19 (2012) 17366–17371.
- 20 [9] H.D. He, W.Z. Lu, Y. Xue, Prediction of PM₁₀ concentrations at urban traffic intersections
21 using semi-empirical box modelling with instantaneous velocity and acceleration, *Atmospheric*
22 *Environment* 43 (2009) 6336–6342.
- 23 [10] W.Z. Lu, Yu. Xue, H.D. He, Detrended fluctuation analysis of particle number concentrations
24 on roadsides in Hong Kong, *Building and Environment* 82 (2014) 580–587.
- 25 [11] H.D. He, W.Z. Lu, Y. Xue, Prediction of particulate matter at street level using artificial neural
26 networks coupling with chaotic particle swarm optimization algorithm, *Building and*
27 *Environment* 78 (2014) 111–117.
- 28 [12] Z. Wang, F. Lu, H.D. He, et al., Fine-scale estimation of carbon monoxide and fine particulate
29 matter concentrations in proximity to a road intersection by using wavelet neural network with
30 genetic algorithm, *Atmospheric Environment* 104 (2015) 264–272.

- 1 [13] Z. Wang, H.D. He, F. Lu, et al., Hybrid model for prediction of carbon monoxide and fine
2 particulate matter concentrations near road intersection, *Transportation Research Record: Journal of the Transportation Research Board* 2503 (2015) 29–38.
- 4 [14] Z. Wang, Q.C. Lu, H.D. He, et al., Investigation of the spatiotemporal variation and
5 influencing factors on fine particulate matter and carbon monoxide concentrations near a road
6 intersection, *Frontiers of Earth Science* 11 (2017) 63–75.
- 7 [15] S. Kaur, M.J. Nieuwenhuijsen, R.N. Colvile, Fine particulate matter and carbon monoxide
8 exposure concentrations in urban street transport microenvironments, *Atmospheric Environment* 41 (2007) 4781–4810.
- 10 [16] S. Kaur, M.J. Nieuwenhuijsen, Determinants of personal exposure to PM_{2.5}, ultrafine particle
11 counts, and CO in a transport microenvironment, *Environmental Science & Technology* 43
12 (2009) 4737–4743.
- 13 [17] X. Jin, L. Yang, X. Du, et al., Particle transport characteristics in the micro-environment near
14 the roadway, *Building and Environment* 102 (2016) 138–158.
- 15 [18] J. Richmond-Bryant, M.G. Snyder, R.C. Owen, et al., Factors associated with NO₂ and NO_x
16 concentration gradients near a highway, *Atmospheric Environment* 174 (2018) 214–226.
- 17 [19] J. Richmond-Bryant, C. Saganich, L. Bukiewicz, et al., Associations of PM_{2.5} and black carbon
18 concentrations with traffic, idling, background pollution, and meteorology during school
19 dismissals, *Science of the Total Environment* 407 (2009) 3357–3364.
- 20 [20] H. Wu, S. Reis, C. Lin, et al., Identifying drivers for the intra-urban spatial variability of
21 airborne particulate matter components and their interrelationships, *Atmospheric Environment*
22 112 (2015) 306–316.
- 23 [21] N.A.H. Janssen, G. Hoek, M. Simic-Lawson, et al., Black carbon as an additional indicator of
24 the adverse health effects of airborne particles compared with PM₁₀ and PM_{2.5}, *Environmental
25 Health Perspectives* 119 (2011) 1691–1699.
- 26 [22] S.S. Park, K.H. Lee, Characterization and sources of black carbon in PM_{2.5} at a site close to a
27 roadway in Gwangju, Korea, during winter, *Environmental Science: Processes & Impacts* 17
28 (2015) 1794–1805.
- 29 [23] S. Hankey, J.D. Marshall, Land use regression models of on-road particulate air pollution
30 (particle number, black carbon, PM_{2.5}, particle size) using mobile monitoring, *Environmental*

- 1 Science & Technology 49 (2015) 9194–202.
- 2 [24] Z. Wang, Characterizing and modeling spatiotemporal distribution of fine particulate matter
3 and black carbon near road intersection, PhD thesis, Shanghai Jiao Tong University, Shanghai,
4 China, 2016. (in Chinese)
- 5 [25] Z. Wang, D. Wang, Z.R. Peng, et al., Performance assessment of a portable nephelometer for
6 outdoor particle mass measurement, Environmental Science: Processes & Impacts 20 (2018)
7 370–383.
- 8 [26] Y. Zhu, W.C. Hinds, S. Kim, et al., Concentration and size distribution of ultrafine particles
9 near a major highway, Journal of the Air & Waste Management Association 52 (2002) 1032–
10 1042.
- 11 [27] Ministry of Ecology and Environment of the People's Republic of China, China Vehicle
12 Emission Control Annual Report,
13 http://www.zhb.gov.cn/gkml/hbb/qt/201601/t20160119_326622.htm, retrieved 17/04/2017.
- 14 [28] T.J. Hastie, R.J. Tibshirani, Generalized additive models, London: Chapman and Hall 1990.
- 15 [29] Y. Gao, Z. Wang, Q.C. Lu, et al., Prediction of vertical PM_{2.5} concentrations alongside an
16 elevated expressway using neural network hybrid model and generalized additive model,
17 Frontiers of Earth Science 11 (2017) 347–360.
- 18 [30] D.C. Carslaw, S.D. Beevers, J.E. Tate, Modelling and assessing trends in traffic-related
19 emissions using a generalized additive modeling approach, Atmospheric Environment 41
20 (2007) 5289–5299.
- 21 [31] J. Richmond-Bryant, L. Bukiewicz, R. Kalin, et al., A multi-site analysis of the association
22 between black carbon concentrations and vehicular idling, traffic, background pollution, and
23 meteorology during school dismissals, Science of the Total Environment 409 (2011) 2085–
24 2093.
- 25 [32] C. Reche, X. Querol, A. Alastuey, et al., New considerations for PM, black carbon and particle
26 number concentration for air quality monitoring across different European cities, Atmospheric
27 Chemistry and Physics Discussions 11 (2011) 6207–6227.
- 28 [33] C.M. Kendrick, P. Koonce, L.A. George, Diurnal and seasonal variations of NO, NO₂, and
29 PM_{2.5}, mass as a function of traffic volumes alongside an urban arterial, Atmospheric
30 Environment 122 (2015) 133–141.

- 1 [34] L. Jian, Y. Zhao, Y.P. Zhu, et al., An application of ARIMA model to predict submicron particle
2 concentrations from meteorological factors at a busy roadside in Hangzhou, China, *Science of
3 the Total Environment* 426 (2012) 336–345.
- 4 [35] A. Belušić, I. Herceg-Bulić, Z.B Klaić, Using a generalized additive model to quantify the
5 influence of local meteorology on air quality in Zagreb, *Geofizika* 32 (2015) 47–77.
- 6 [36] W.M. Yang, L.G., Ying, Atmospheric stability and air pollution in Shanghai, *Chinese Journal
7 of Environmental Engineering* 7 (1986) 47–52. (in Chinese)
- 8 [37] A.R. Chughtai, M.E. Brooks, D.M. Smith, Hydration of black carbon, *Journal of Geophysical
9 Research Atmospheres* 1011 (1996) 19505–19514.
- 10 [38] H. Wang, Q. He, Y. Chen, et al., Characterization of black carbon concentrations of haze with
11 different intensities in Shanghai by a three-year field measurement, *Atmospheric Environment*
12 99 (2014) 536–545.
- 13 [39] J.L. Pearce, J. Beringer, N. Nicholls, et al., Quantifying the influence of local meteorology on
14 air quality using generalized additive models, *Atmospheric Environment* 45 (2011) 1328–1336.
- 15 [40] M. Jamriska, L. Morawska, K. Mergersen, The effect of temperature and humidity on size
16 segregated traffic exhaust particle emissions, *Atmospheric Environment* 42 (2008) 2369–2382.
- 17 [41] N. Pérez, J. Pey, M. Cusack, et al., Variability of particle number, black carbon, and PM₁₀,
18 PM_{2.5}, and PM₁ levels and speciation: Influence of road traffic emissions on urban air quality,
19 *Aerosol Science and Technology* 44 (2010) 487–499.
- 20 [42] R.H. Zhang, Y.B. Ma, F. You, et al., Exploring to direct the reaction pathway for hydrogenation
21 of levulinic acid into γ -valerolactone for future Clean-Energy Vehicles over a magnetic Cu-Ni
22 catalyst, *International Journal of Hydrogen Energy* 42 (2017) 25185–25194.
- 23 [43] R.H. Zhang, Z.C. He, H.W. Wang, et al., Study on self-tuning tyre friction control for
24 developing main-servo loop integrated chassis control system, *IEEE Access*, 5 (2017) 6649–
25 6660.

Fine-scale variations in PM_{2.5} and black carbon concentrations and corresponding influential factors at an urban road intersection**Highlights**

- Three-point synchronous observations are conducted at a road intersection.
- PM_{2.5} varies similarly at sites but BC more syncs with the diurnal traffic cycle.
- Background site explains 77–99% of the variance in $\ln(PM_{2.5})$ but 33–43% in $\ln(BC)$.
- Meteorological parameters influence the PM_{2.5} or BC variation in different ways.
- Traffic contributes more to the short-time variation of BC than that of PM_{2.5}.